Supplementary material

Part A: *LTMLD –Lagged Time Mixed Layer Depth - Method*

This method uses a vertical density profile, ρ(z), at a given date and time (t_p), and net surface heat and water fluxes at the same geographical position, together with a specific window of time *win* before the date of the density profile (t_p). Surface buoyancy fluxes are calculated using:

$$J_b = g\ \alpha Q_{net}/(\rho_s\ C_p) + g\ SSS\ \ \beta\ Q_e\ /(\rho_s\ L_v)$$

where J_b is the buoyancy flux (in $m^2 s^{-3}$) from the atmosphere to the ocean, Q_{net} and Q_e are, respectively, the net heat and water fluxes modifying salinity (in W m^{-2}), ρ_s is surface water density, *SSS* is sea surface salinity, C_p and L_v are specific heat capacity and latent heat coefficients, and g is the gravity acceleration (Gill 1982, d'Ortenzio and Prieur, 2011). The terms α and β are the thermal and the salinity expansion coefficients for seawater, and are represented by:

$$\alpha = -\ (1/\rho_s)\ \partial\rho_s/\partial SST$$

$$\beta = \ \ (1/\rho_s)\ \partial\rho_s/\partial SSS$$

where *SST* is the sea surface temperature (°C) and *SSS* the sea surface salinity (PSU). The time window *win* [t_i ,t_p] before the observation time t_p is fixed, where t_i is anterior to t_p. For example, t_i could be chosen as t_p-1 day, or t_p- 3 days so that *win* encompasses some anticipated maximum MLD for 1 or 3 days before t_p, or even t_p-200 days when the aim is to retrieve maximum Winter MLD several months before t_p.

The temporally cumulated surface buoyancy flux [cumJb(t)] for *win* is then calculated, and the time (t_m), the value of cumJb(t_m), of minimum cumJb(t) inside the temporal window, and cumJb(tp) are found.

BI(z) is the vertical profile of integrated buoyancy from the profile of ρ(z) at time t_p, which is calculated for any depth -h as follows :

$$BI(h) = \left(g \middle/ \rho 0\right).\int_{-h}^{0}(\rho(h) - \rho(z))dz$$

where ρ0 is any constant density reference near the density range of ρ(z). BI is the buoyancy integral of the measured buoyancy profile.

The LTMLD (t_m, t_p) value is obtained from the equation:

$$BI(LTMLD) = cumJb(t_p) - cumJB(t_m),$$

where LTMLD is the lagged time mixed layer depth. This equation states that the amount of excess buoyancy brought by the atmosphere since time t_m down to the ocean has increased the oceanic buoyancy content at the location of the measured density profile. BI(LTMLD) corresponds to this amount, on condition, however, that advection of buoyancy is negligible for the time window *win*.

The above procedure proceeds with a retrograde window (i.e. $t_i<t_p$).

In the particular case where LTMLD is sought for a time after the date of the profile (prograde), *win* is chosen as the temporal window $[t_p,t_i]$, which means that the excess buoyancy contained in the ocean at t_p is lost through the atmosphere because of the accumulation of negative Jb between t_p and t_m. In both prograde and retrograde cases, the vertical profile ρ(z) observed at time t_p is more buoyant than one which might have been observable at time t_m.

Since density increases with depth, BI(h) is always positive. Thus, the depth profile will be more 'buoyant' at t_m than at t_p, and so the ocean becomes stratified or unstratified during the period [t_m, t_p].

However, the value found for LTMLD cannot be the real, value that might have been observable at time t_m, because the method does not take into account changes in density profiles due to advection. Nevertheless, use of this method has been found to give realistic values of MLD (Prieur et al. 2010, Contract report). In Figure 7, the winter mixed layer depths (W-MLD) in 2008 were calculated with a window of 200 days using ECMWF surface fluxes for each cast of the section. Indeed, the W-MLDs found correspond very closely to the top depth of the nutricline and were deeper for casts inside the eddies than for those outside. The W-MLD was also fairly close to the depth where AOU is nil or weak. This can be interpreted as one indication of winter ventilation of depths less than W-MLD and with a positive net production for the *win* period. At depths above W-MLD, the net production is negative and AOU starts to increase with depth.

MLD_{2d} has another signification, which is to define the maximum mixing depth that might have been measured in a time window of 3 days before the measurement (t_p – 3days, t_p). Indeed, MLD_{2d} values were similar to the maximum $MLD_{0.03}$ values measured every 3 hours during LD station occupation, given that the MLD_{2d} method was applied for the last cast of each LD station A, B and C.

This work was funded by Mercator-Coriolis PROSAT Grant n° Ifremer 08/ 2 210 118

Part B Simulation of an eddy

The objectives are to specify the fitting method used to simulate observed eddy structure during the BOUM experiment through use of an idealized structure, to show some of the characteristics and dynamical properties of the eddies, and to evaluate the quality of the fit by comparing observed and simulated fields particular to eddy A.

Eddy Equations

In cylindrical coordinates (r, φ, z), a circular, stationary, geostrophic eddy with vertical axis and velocity gradient ($v_r = 0$, v_φ, $v_z = 0$) satisfies the following equations (Brenner et al., 1993):

$$v_\varphi^2/r + f\, v_\varphi = (1/\rho_r)\, \partial p/\partial r = f v_g \qquad (1)$$

$$\partial p/\partial z = -g\, \rho(r,z) \qquad (2)$$

$$f \partial v_g/\partial z = -(1/\rho_r)\, \partial \rho/\partial r \qquad (3)$$

Equation (1) is the radial-moment equation, where f is the Coriolis parameter, p is pressure, v_g is geostrophic velocity and ρ_r is a constant reference density. The second equation in (1) states only the geostrophic equilibrium and shows that geostrophic velocity v_g is different from gradient velocity due to cyclostrophic acceleration. Equation (2) accounts for the use of hydrostatic approximation. Equation (3) is the conventional wind thermal equation which links velocity to density fields.

Other dynamical quantities are the vertical relative vorticity component ζ and Ertel potential vorticity Q, when the two horizontal components of vorticity are nil or negligible and N^2 is the Bünt Vaîssala frequency:

$$\zeta = (1/ r)\, \partial(r v_\varphi)/\partial r$$

$$Q = f\,N^2\,(1 + \zeta/f)/g$$

$$N^2 = -(g/\rho_r)\,\partial\rho/\partial z$$

A measurement of the non-linearity of an eddy is given by the standard Rossby number for eddies

Ro $=|\zeta_{min}|/f$. Ro typically ranges from 0.20 to 0.60 for coherent anticylonic vortex (Brenner et al., 1993, Pingree and Le Cann, 1992)

A simple analytical velocity $v_\varphi(r, L)$ summarizing an idealized structure for BOUM eddies is a Rayleigh distribution on a horizontal plane (Pingree and Le Cann, 1993).

$$v_\varphi = \omega\, r \exp(-r^2/L^2)\ ;\ v_r = 0\ ;\ (4)$$

where ω is rotation pulsation ($\omega = 2\pi/Tr$, Tr rotation period) and L is a distance, here called Rayleigh distance. ω is negative for an anticyclonic eddy in the Northern hemisphere.

$$\psi = -\,\omega(L^2/2)\exp(-r^2/L^2) \quad (5)$$

such as $v_\varphi = \partial\psi/\partial r$. ($\psi>0$ when $\omega<0$). Using a stream function ψ_g such as $v_g = \partial\,\psi_g/\partial r$ and a without dimension parameter ψ_{cor}, the combination of equations (1), (4) and (5) gives an expression for ψ_{cor}:

$$\psi_g = \psi.\,\psi_{cor} \quad (6)$$

$$\psi_{cor} = [1 + (\omega/2f)\exp(-r^2/L^2)\,] \quad (7)$$

Near to an anticyclonic eddy axis, $\psi_{cor} < 1$, and the geostrophic stream function is flatter than the gradient stream function. When r>>L, both are equal.

Figure SM1 shows an example of radial variations at z= constant of $f\psi$ (in black, Top panel) and $f\,\psi_g$ (red). The azimuthal velocity gradient (middle panel) is always negative, decreasing linearly as ωr to $r \sim L/3$, minimum at $r = L/\sqrt{2}$ and increases further towards 0. Relative vorticity scaled by f (bottom panel) is minimum near the axis and equal to $Ro = -\zeta/f$, then increases between r = 0 and r = L. Following this last r value, the relative vorticity is positive, reaches a maximum at $r = L\sqrt{2}$, and then decreases towards 0.

Table SM1 shows the numerical value for the different characteristic values of r scaled by L and corresponding Vaz ($= v_\varphi$) values scaled by ωL. Vo is hereafter defined as ωL for convenience.

Fitting an idealized structure to observed eddies

It is necessary to adjust ω and L in order to obtain a idealized 3D structure of an observed eddy. In the adjustment, ω is assumed to be constant with depth, and L variable, L=L(z).

Similar adjustments have already been applied, for example by Pingree and Le Cann (1993) who used geostrophic calculations and measured velocities from drogued buoys and/or VMADCP. An example of adjustment with the method proposed here is presented for eddy A. A complete eddy A work map is presented in Figure SM2 (Top). Locations of VMADCP measurements are indicated (blue line, see also Figure 8). As the depth ranges of correct horizontal velocity measurements were strongly variable, the ESE-WNW XBT section was used to compare simulated and observed Vaz. This section crosses the eddy approximately along a diameter and observations of the maximum radial velocity range 30-40 cm s^{-1} and $|Vaz|_{max}$ was chosen as 33 cm s^{-1} at 60 m depth. A second sort of information from observations is the vertical profile of the geopotential difference δG(z) between the cast near the centre of eddy (cast 147) and the outer cast 130. A South to North nine-cast CTD section A (marked in thick red in Figure SM2) was performed, starting with cast 147 the day following the XBT section described above and near to the presumed location of the eddy centre. This CTD section (A) was prolonged by a section at this northern tip in order to reach a virtual cast 130', at the same distance from eddy center (120 km) than cast 130. Data from cast 130 has been used at cast 130' assuming eddy circular axis symmetry.

The vertical density profiles for both casts 147 and 130 are seen superimposed in Figure SM2 (bottom), with vertical profiles of density anomaly and the δG(z) profile calculated from T and S profiles. The maximum of δG(z) was also observed at 60 m.

ω and L(z) were then calculated in 2 steps. First, ω was calculated and second, the profile of L(z) using 2 expressions was determined from equations (5), (6) and (7) :

at r=0 :

$$f\,\psi_g(r=0,z) = \delta G(z) = f\,\omega(L^2/2).\,[1+(\omega/2f)]\,, \qquad (8)$$

as Vo= ωL:

$$fVo(z)L(z)[1+(Vo/2fL)] = \delta G(z) \qquad (8b)$$

and

$Vo = - |Vaz|_{max}/0.429$ at z= depth of max[δG(z)] (9)

Relation (9) is determined using Table SM1

step 1

For z= 60 m where δG(z) and |Vaz| are maximum, let:

V= -|Vaz|max

G= max[δG(z)]

ω is then calculated using equations (8) and (8b)

Vo = V/0.429 ; using table SM1 for r= L/√2

$L = - (1/fVo)[4G+Vo^2]/2$; using equation (8b)

ω = Vo/L

step 2:

L(z) is calculated using found ω and equation (8).

Then, v_φ -using equation (4)- and ζ can be obtained at any r and z as can v_g using equation (1).

The simulated density field is required to calculate potential vorticity Q. This was achieved by using the "out" profile of cast 130 at r_o =130 km and a numerical horizontal integration from r_o to any r using equation (3). All numerical calculations were performed on a grid spacing of 2 km on r and 10 m on z.

Potential vorticity could then be calculated.

Results

Eddy A was simulated as described above with -1.8181 e-05 s^{-1} , which corresponds to Tr= 4 days using δG(z) profile of Figure SM2 and G= 1.26 m^2s^{-2} ; f=9.1531e-05 s^{-1} ; V=- 32 cm s^{-1} at 60 m. The Rossby number Ro was found to be as high as 0.3973, which corresponds to a relatively high importance of cyclostrophy and the coherent vortex nature of Eddy A.

Figure SM3 shows along-diameter sections of idealized structure for azimuthal velocity (upper left, drawn as <0 when ingoing the figure and >0 when outgoing), σ_θ (upper right), ζ/f (bottom left) and absolute potential vorticity (Bottom right). For clarity, the section ranges from -70 to 70 km on the X-axis. On each graph can be seen the representative loci of

maximum of absolute azimuthal velocity (dotted), and null and maximum relative vorticity (solid and dashed lines, respectively) . Isopycnal lines are seen to deepen toward the axis by approximately ΔH = 100 m for a range of σ_θ 28.2 -29 kg m^{-3}, but when looking at lower σ_θ, ΔH decreases and even changes sign near 50 m, where isopycnal 27.5 is flat, as anticipated from density profiles in Figure 2SM. In the narrow, 20-50 m depth range , the density in the eddy core is higher than it is outside. Such a feature has already been observed for deep anticylonic eddies as well as for meddies and also for swoddies (Pingree and Le Cann , 1992) and was theoretically explained by differential heating /cooling by Chapman and Nof (1988). The ζ/f graph also clearly shows the envelope of maximum relative vorticity which crosses through the density lines on σ_θ , thus forming a barrier of potential vorticity which separates the inner part of the eddy from the outer part horizontally and along the isopycnal, due to a maximum of Q.

Figure SM4 compares the azimuthal velocity field (left) and density field as they were observed (black isolines) superimposed upon the oxygen field (Top) and according to simulations (Bottom). On the right, only the radius sections which correspond to the observed section A have been drawn. Simulated and observed velocity sections show similar patterns, both for amplitude and depth, even if on observed ADCP sections some dissymmetry in maximum amplitude was noted. The differences remain minor (5-7cm s^{-1}) and can be explained by inertial internal waves, errors in ADCP velocities (circa +-2 cm s^{-1}), possible drifting of the eddy centre (2-5 cm s^{-1}) and by possible ringing of the eddy. The reconstitution is fairly close to what was observed. The deepening of isopycnals is also quite similar. The bigger, although still moderate, discrepancies appear from range 20-40 km to depth. However, the pycnostads 28.1-28.2 kg m^{-3} at 130-170 m and nearly 28.6 kg m^{-3} at 200-250 m are retrieved near the axis in the simulated field. In fact, the reconstituted and observed density profiles for r = 0 (not shown), are similar (difference less than 0.02 kg m^{-3}) due to the use of observed geopotentials in the procedure. This can be the case only when highly accurate $\delta G(z)$ is available.

The barrier effect of potential vorticity maximum is marked when looking at the observed oxygen field. Strong horizontal gradients are evidenced between solid and dashed lines, while outside of this slanting band the oxygen concentrations are quite homogeneous even if some vertical gradient can be noted. The core of the eddy is not a fully homogeneous body of water due to residual stratification, even if it is isolated from the outer part of the eddy. Some

drawing discrepancies are visible and have been attributed to the interpolation method between the end of the real section A (at 55 km; real casts are marked by a white cross and the virtual cast 130).

Because the observed data fitted well with the idealized eddy structure, it was possible to determine the Rossby number, ζ/f, which is a characteristic number for each eddy. The Rossby number evidences the shape of the inner part of eddy A, isolated from the outer part. Comparable simulations were performed for eddies B and C. The first results are not as accurate as for eddy A, and are reported in Table 3. Recorded velocities at LD B and C by ADCP were lower than for eddy A, and the influences of internal near-inertial waves and drifting of eddy centres could have been greater. Future work is needed to optimize the fitting and to find more accurate ω by taking ARGO float trajectories and profiles for these eddies into account.

Table SM1

	Solid limit Rsol	Max$\|V_{az}\|$ $R_{Vaz\ max}$	$\zeta = 0$ R_{core}	Max ζ R_{ζ}	 R_{tot}
r	0.333 L	0.707L	L	1.414L	2L
V_{az}	$0.333\omega L\ e^{-0.11}$	$0.707\omega L\ e^{-0.5}$	$\omega L\ e^{-1}$	$1.414\ \omega L\ e^{-2}$	$2\omega L\ e^{-4}$
V_{az}	0.299 ωL	0.429 ωL	0.378 ωL	0.1914 ωL	0.0366 ωL

Table SM1: Numerical values of different characteristic values of r scaled by L, and corresponding Vaz (= v_{φ}) values scaled by ωL using the Rayleigh model.

Figure captions :

Figure SM1: Examples of radial variations of $f\psi$ (red) and $f\psi_g$ (red) for a Rayleigh eddy simulation, using L = 25 km, Tr = 5.5 days (Top), azimuthal velocity Vaz (Middle) and ζ/f ratio (Bottom). The x-axis spans the 0-80 km range along an eddy radius. The 3 * on each graph marks the distances $L/\sqrt{2}$, L and $L\sqrt{2}$, where Vaz (<0) reaches an extremum, $\zeta = 0$ and ζ is maximum, respectively. Units are indicated in brackets in the titles.

Figure SM2: Map of work, eddy A (Top). The 4-day ship track between casts 130 and 187 is indicated as a solid blue line with dashed arrows. Numbers given refer to the cast numbers cited in the text. Pink lines correspond to section A with observed (thick) and prolonged (dashed) parts (see text). Bottom: from left to right, σ_θ, anomaly $\delta\sigma_\theta$ and $\delta G(z)$ respectively. On the left, a vertical black line indicates the isopycnal deepening ΔH of the density observed at the negative maximum of $\delta\sigma_\theta$ depth. Horizontal black dashed and solid lines, respectively, depict the top and bottom of density anomaly in the middle panel. The top of anomaly $\delta\sigma_\theta$ corresponds to the depth of a maximum of δG (right) and the intersection of the two σ_θ (z) (left).

Figure SM3: Eddy A, Rayleigh simulation.

Figure SM4: Comparison for eddy A between observed (Top) and simulated (Bottom) fields.

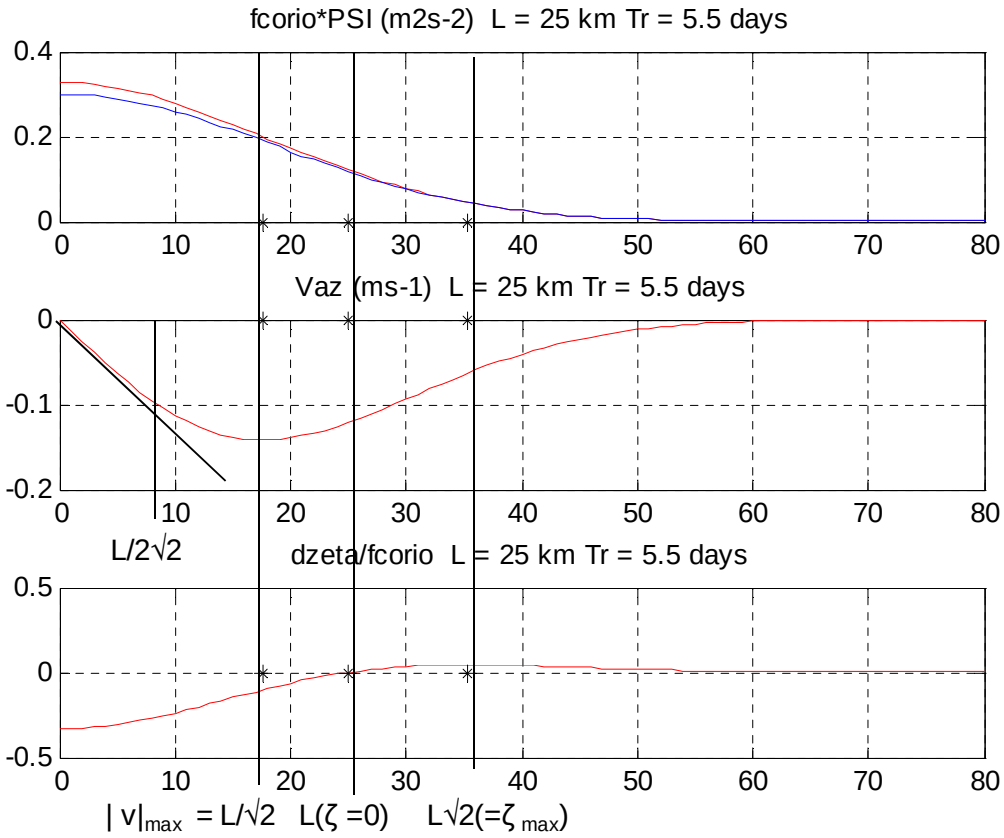

Figure SM1 Moutin et al.

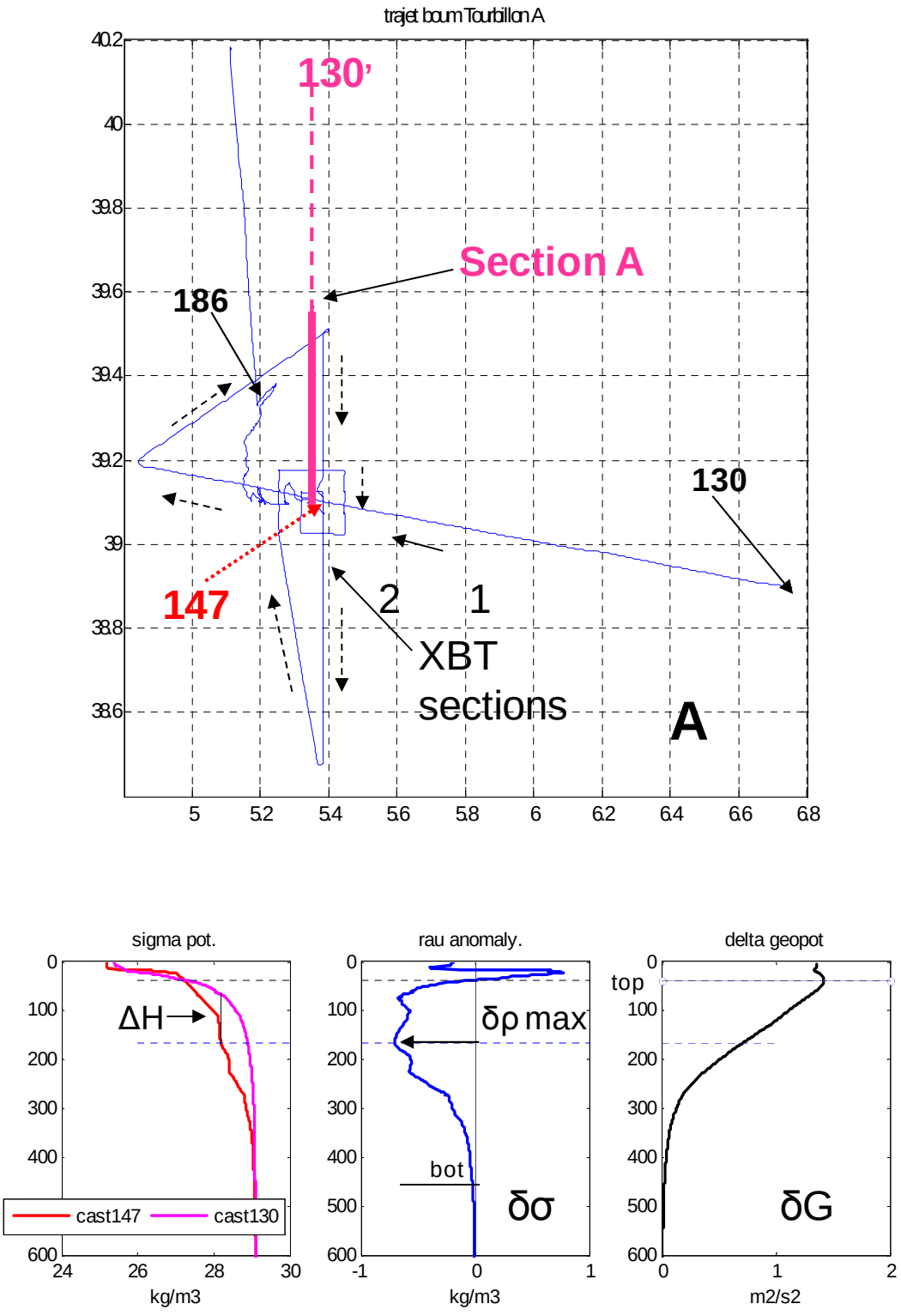

Figure SM2 Moutin et al.

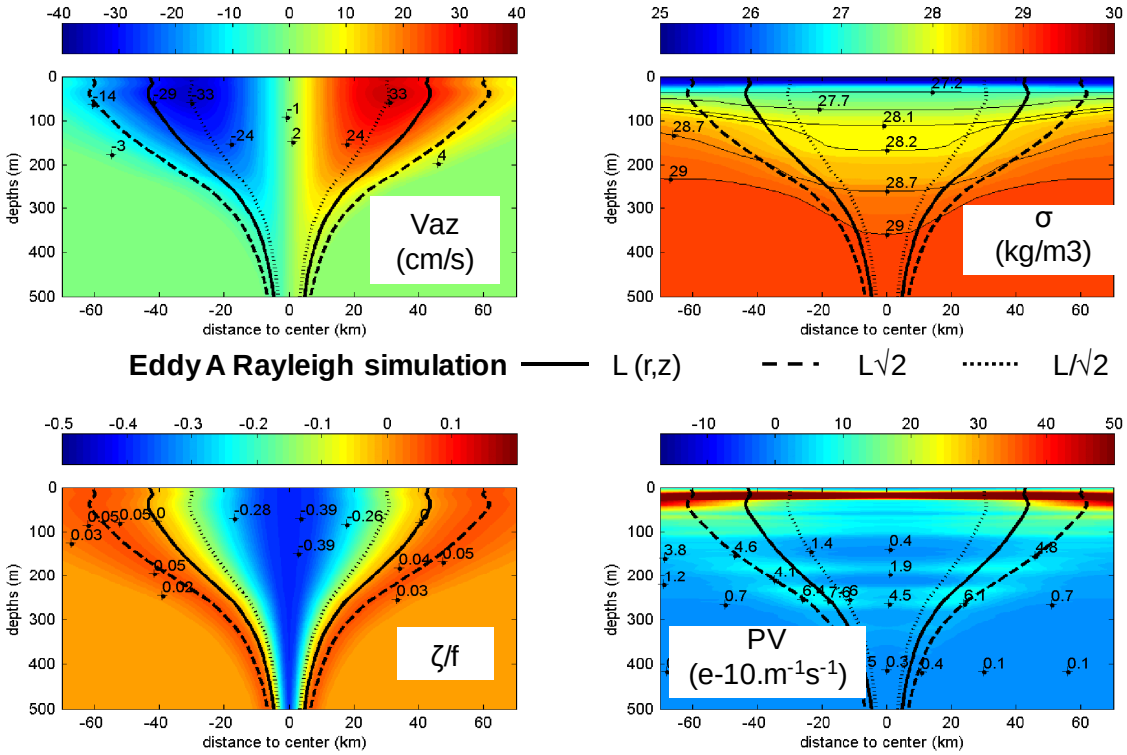

Figure SM3 Moutin et al.

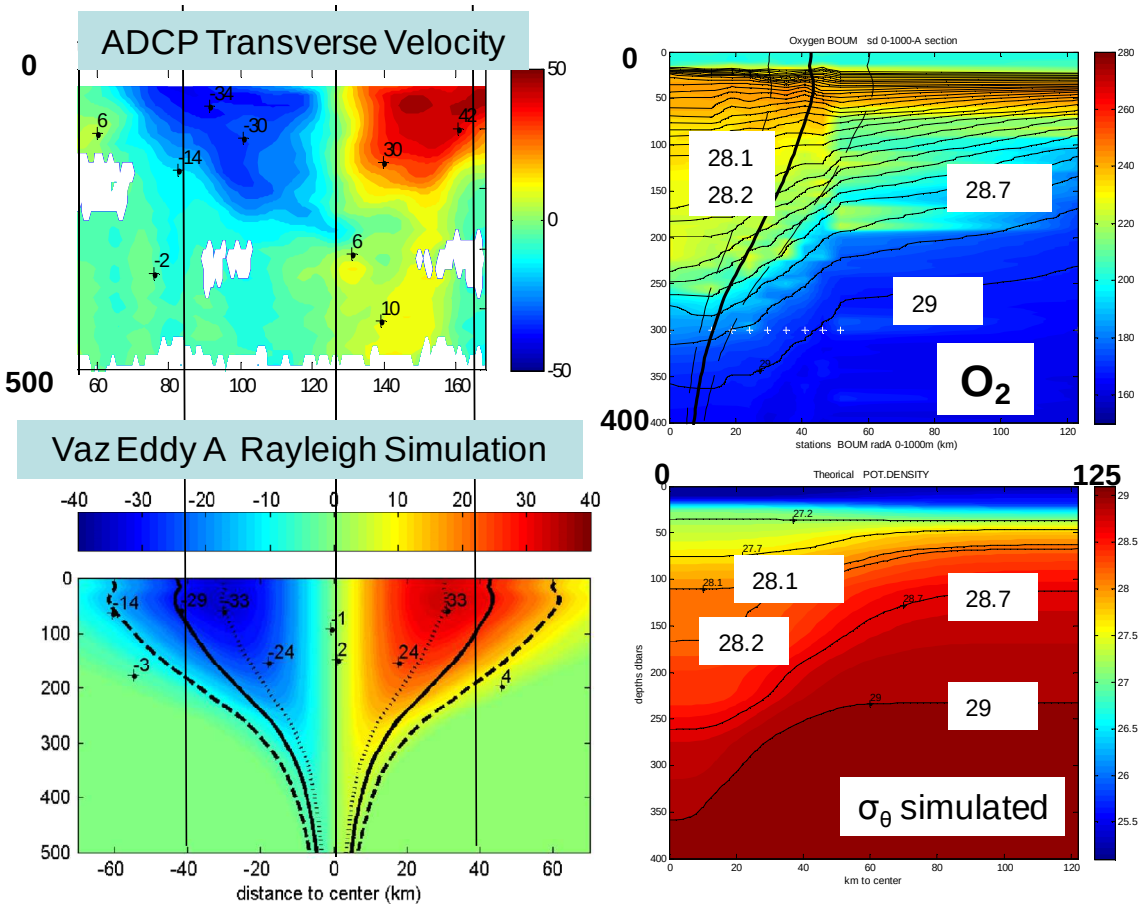

Figure SM4 Moutin et al.